The poroelastic layer with an axisymmetric cylindrical hole under different types of loading

Natalya Vaysfeld and Zinaida Zhuravlova

Abstract. The exact solution of the poroelastic axisymmetric problem for a layer with a cylinderical hole is constructed under assumptions of Biot's model. The calculations provided by derived explicit formulas for full stress and pore pressure allow to state some important dependencies between the poroelastic stress state of the layer and type of poroelastic materials, loading types and height of the layer.

1. Introduction

Poroelasticity investigates the interaction between fluid flow and solid deformation within porous materials, making it a crucial field of study in geomechanics, biomedicine, and civil engineering. The poroelastic layers with cylindrical holes have plenty of real-world applications: the analysis of stress and deformation in soil layers with boreholes, the study of fluid flow around cylindrical inclusions in biological tissues, the assessment of seepage and consolidation behavior in geotechnical engineering applications. There are various experimental techniques employed to investigate poroelastic layers with cylindrical holes: laboratory experiments, such as permeability measurements, consolidation tests, and imaging techniques like MRI and X-ray CT scanning. Meanwhile conducting experiments in complex porous media systems is a big challenge, so the modeling of such structures and investigation of their properties is an extremely relevant task.

The numerical methods like finite element analysis and boundary element methods are widely used to solve poroelasticity problems. The problem of multi-scale characterization and optimization of absorption properties of

poroelastic materials was studied in [6] with the help of asymptotic homogenization method and optimization procedure. The modeling for a more realistic description of a thermo-poro-elastic source and the embedding medium was done in [11]. For this aim a numerical method to represent inclusions with an arbitrary geometry was proposed. A new algorithm based on the spectral method for the computation of Stoneley wave dispersion and attenuation propagating in cylindrical structures composed of fluid, elastic and poroelastic layers was proposed in [8]. The Haar wavelet discrete transform, the artificial neural networks (ANNs), and the random forests were applied in [7] to predict the location and severity of a crack in an Euler–Bernoulli cantilever subjected to the transverse free vibration.

However, the numerical methods have some limitations, because they cannot give a complete qualitative picture of porous stress distribution as in corner points or at tips of a crack. That is why semi-analytical and analytical methods are still relevant. The acoustic response of a rigidly backed poroelastic layer with a periodic set of elastic cylindrical inclusions embedded was studied in [17] by a semi-analytical approach, based on Biot's theory to account for the deformation of the skeleton, coupling mode matching technique, Bloch wave representation, and multiple scattering theory. A simple method to discuss the horizontal dynamic response of the cylindrical rigid foundation partially embedded in a poroelastic soil layer was proposed in [18] by virtue of Biot's elastodynamic model. It was based on the Novak plane strain model, the assumption of foundation end soil as a continuous medium of finite thickness, and adopting Newton's second law. Analytical solutions of the problem on dynamic stress concentration and the surface displacement of a partially debonded cylindrical inclusion in the covering layer under the action of a steady-state horizontally polarized shear wave were presented in [13]. It was shown in [9] that low frequency performance could be significantly improved by embedding periodically arranged resonant inclusions (slotted cylinders) into the porous matrix. A parametric study was performed there, numerical and semi-analytical calculations were provided. An analytical approach to study the impact of discontinuities and boundary conditions on the critical buckling load and critical stress of nanobeams was developed in [1]. The analytical solution for the axisymmetric problem for a poroelastic solid cylinder was derived in [15] with the help of integral transform method and matrix differential calculation. Some analytical methods from elasticity theory might be interesting by their possible adaptation for poroelasticity problems (see [2], [5]).

Analysis of articles dedicated to the stress state of the layer weakened by defects of different form has shown essential lack of analytical approaches for solving the indicated problem. The authors in the present paper propose to use a new analytical approach that allows to derive the exact solution of the axisymmetric poroelasticity problem for a layer with a cylindrical hole.
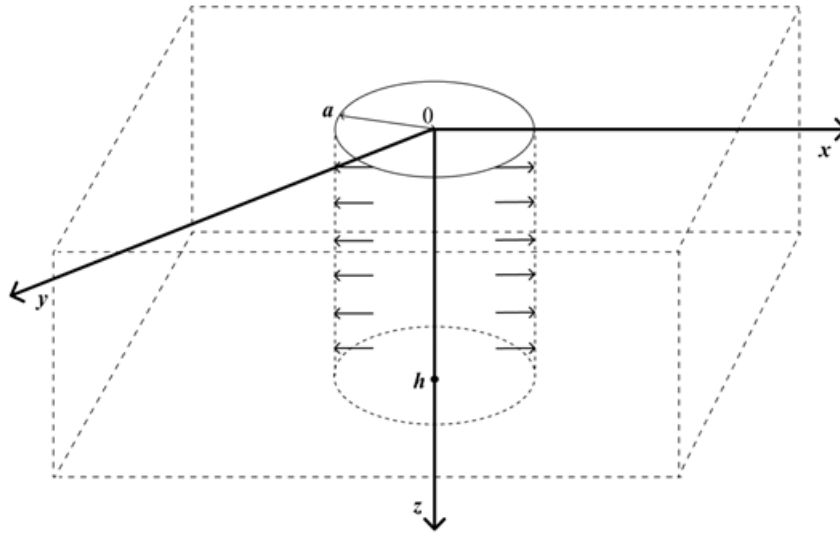
FIGURE 1. The statement of the problem. The axisymmetric cylindrical hole of the radius a and height h with applied stress.

2. The problem's statement

The poroelastic layer ($1 < r < \infty, 0 < z < h$, here r, z is the cylindrical coordinate system) (Figure 1) containing an axisymmetric cylindrical hole is considered in the terms of Biot's model. Biot's model of a poroelastic medium is physically and geometrically linear, that is, it corresponds to the case of small deviations of the field that describe the state of the medium from their equilibrium reference values. According to [3], the main properties of this model are the following: isotropy of the material, reversibility of stress-strain relations under final equilibrium conditions, linearity of stress-strain relations, small strains, the water contained in the pores is incompressible, the water may contain air bubbles, the water flows through the porous skeleton according to Darcy's law.

The ideal contact conditions are fulfilled at the upper and bottom surfaces of the layer:

$$w|_{z=0} = 0, \tau_{rz}|_{z=0} = 0, p|_{z=0} = 0,$$
$$w|_{z=h} = 0, \tau_{rz}|_{z=h} = 0, p|_{z=h} = 0. \tag{1}$$

Here $w = u_z(r, z)$ is dimensionless displacement of the solid skeleton, $\tau_{rz}(r, z)$ is dimensionless tangential effective stress, $p(r, z)$ is dimensionless pore pressure.

On the cylindrical surface the mechanical load with the fluid pressure load is applied:

$$\sigma_r|_{r=1} = L(z) - \alpha P(z), \tau_{rz}|_{r=1} = T(z), p|_{r=1} = P(z), \qquad (2)$$

where $\sigma_r(r, z)$ is dimensionless normal effective stress, α is Biot's coefficient and $L(z), T(z), P(z)$ are given functions.

The system of equilibrium and storage equations has the following form (see [16]):

$$\begin{cases} \frac{1}{r}\frac{\partial}{\partial r}\left(r\frac{\partial u}{\partial r}\right) - \frac{1}{r^2}u + \frac{\kappa-1}{\kappa+1}\frac{\partial^2 u}{\partial z^2} + \frac{2}{\kappa+1}\frac{\partial^2 w}{\partial r\partial z} - \alpha\frac{\kappa-1}{\kappa+1}\frac{\partial p}{\partial r} = 0, \\ \frac{1}{r}\frac{\partial}{\partial r}\left(r\frac{\partial w}{\partial r}\right) + \frac{\kappa+1}{\kappa-1}\frac{\partial^2 w}{\partial z^2} + \frac{2}{\kappa-1}\frac{1}{r}\frac{\partial}{\partial r}\left(r\frac{\partial u}{\partial z}\right) - \alpha\frac{\partial p}{\partial z} = 0, \\ \frac{1}{r}\frac{\partial}{\partial r}\left(r\frac{\partial p}{\partial r}\right) + \frac{\partial^2 p}{\partial z^2} - \frac{\alpha}{K}\left[\frac{1}{r}\frac{\partial}{\partial r}\left(ru\right) + \frac{\partial w}{\partial z}\right] - \frac{S_P}{K}p = 0. \end{cases} \qquad (3)$$

Here $u = u_r(r, z)$ is dimensionless displacement of the solid skeleton, $\kappa = 3 - 4\mu$ is Muskhelishvili's constant, μ is Poisson ratio, $K = 1/Gk, S_P = S_p G, S_p$ is storativity of the pore space, k is permeability, G is shear modulus.

The displacements $u(r, z), w(r, z)$, stress $\sigma_r(r, z), \sigma_z(r, z), \tau_{rz}(r, z)$ and pore pressure $p(r, z)$ that satisfy system (3) with boundary conditions (1)–(2) should be found.

3. The solving method

The original boundary value problem is reduced to the one-dimensional problem with the help of finite sin-, cos-Fourier transform with respect to the variable z:

$$\vec{y}_\beta(r) = \begin{bmatrix} u_\beta(r) \\ w_\beta(r) \\ p_\beta(r) \end{bmatrix} = \int_0^h \begin{bmatrix} u(r, z) \\ w(r, z) \\ p(r, z) \end{bmatrix} \begin{bmatrix} \cos\beta z \\ \sin\beta z \\ \cos\beta z \end{bmatrix} dz, \ \beta = \frac{\pi n}{h}, n = 0, 1, 2, \cdots$$

The derived one-dimensional problem in transform's domain is formulated as the vector boundary value problem:

$$\begin{cases} L_2\vec{y}_\beta(r) = 0, 1 < r < \infty, \\ A_\beta\vec{y}'_\beta(1) + B_\beta\vec{y}_\beta(1) = \vec{g}_\beta, \end{cases} \qquad (4)$$

where

$$L_2 = \begin{pmatrix} \frac{1}{r}\frac{d}{dr}\left(r\frac{d}{dr}\right) - \frac{1}{r^2} - \frac{\kappa-1}{\kappa+1}\beta^2 & \frac{2\beta}{\kappa+1}\frac{d}{dr} & -\alpha\frac{\kappa-1}{\kappa+1}\frac{d}{dr} \\ \frac{2\beta}{\kappa-1}\frac{1}{r}\frac{d}{dr}(r) & \frac{1}{r}\frac{d}{dr}\left(r\frac{d}{dr}\right) - \frac{\kappa+1}{\kappa-1}\beta^2 & \alpha\beta \\ -\frac{\alpha}{K}\frac{1}{r}\frac{d}{dr}(r) & -\frac{\alpha\beta}{K} & \frac{1}{r}\frac{d}{dr}\left(r\frac{d}{dr}\right) - \beta^2 - \frac{S_P}{K} \end{pmatrix}$$

is the differential operator of the second order, and

$$A_\beta = \begin{pmatrix} \frac{\kappa+1}{2\kappa-2} & 0 & 0 \\ 0 & 1 & 0 \\ 0 & 0 & 0 \end{pmatrix}, B_\beta = \begin{pmatrix} \frac{3-\kappa}{2\kappa-2} & \frac{3-\kappa}{2\kappa-2}\beta & 0 \\ -\beta & 0 & 0 \\ 0 & 0 & 1 \end{pmatrix}, \vec{g}_\beta = \begin{pmatrix} \frac{L_\beta}{2} - \alpha P_\beta \\ T_\beta \\ P_\beta \end{pmatrix}.$$

The vector boundary value problem (4) is solved with the help of matrix differential calculation (see [15], [10]). According to this method, the corresponding matrix differential equation

$$L_2 Y_\beta(r) = 0 \tag{5}$$

is considered. Here $Y_\beta(r)$ is a 3×3 matrix. The correspondence $L_2 H(r, \xi) = -H(r, \xi) M(\xi)$ (see [12]) is used, where

$$H(r, \xi) = \begin{pmatrix} Y_1(\xi r) & 0 & 0 \\ 0 & Y_0(\xi r) & 0 \\ 0 & 0 & Y_0(\xi r) \end{pmatrix},$$

$Y_0(\xi r), Y_1(\xi r)$ are Bessel functions of the second kind, and

$$M(\xi) = \begin{pmatrix} \xi^2 + \frac{\kappa-1}{\kappa+1}\beta^2 & \frac{2\beta}{\kappa+1}\xi & -\alpha\frac{\kappa-1}{\kappa+1}\xi \\ \frac{2\beta}{\kappa-1}\xi & \xi^2 + \frac{\kappa+1}{\kappa-1}\beta^2 & -\alpha\beta \\ \frac{\alpha}{K}\xi & \frac{\alpha\beta}{K} & \xi^2 + \beta^2 + \frac{S_P}{K} \end{pmatrix}.$$

The solution of the matrix differential equation (5) (see [6]) is given by the formula

$$Y_\beta(r) = \frac{1}{2\pi i} \oint_C H(r, \xi) M^{-1}(\xi) d\xi, \tag{6}$$

where $M^{-1}(\xi)$ is the inverse matrix to $M(\xi)$, the closed contour C covers all singularity points of the matrix $M^{-1}(\xi)$, which are $\xi = \pm i\beta, \xi = \pm i\sqrt{\frac{\frac{\alpha^2(\kappa-1)}{\kappa+1}+S_P}{K} + \beta^2}$. Calculation of the contour integral (6) was done with the help of residual theorem. The system of fundamental matrix solutions $Y_i(r), i = \overline{1,4}$ is derived. The solution of the vector boundary value problem (4) can be written in the form

$$\vec{y}_\beta(r) = (Y_1(r) + Y_3(r)) \begin{pmatrix} c_1 \\ c_2 \\ c_3 \end{pmatrix}, \tag{7}$$

where $c_i, i = \overline{1,3}$ are constants found from the boundary conditions in (4). Note that the solution (7) corresponds to the case $\beta \neq 0$.

The case when $\beta = 0$ is considered separately. In this case the vector $\vec{y}_0(r)$ has the form $\vec{y}_0(r) = \begin{pmatrix} u_0(r) \\ p_0(r) \end{pmatrix}$, and the problem (5) can be written as

$$\begin{cases} \tilde{L}_2 \vec{y}_0(r) = 0, 1 < r < \infty, \\ A_0 \vec{y}_0'(1) + B_0 \vec{y}_0(1) = \vec{g}_0. \end{cases} \tag{8}$$

Here

$$\tilde{L}_2 = \begin{pmatrix} \frac{1}{r}\frac{d}{dr}\left(r\frac{d}{dr}\right) - \frac{1}{r^2} & -\alpha\frac{\kappa-1}{\kappa+1}\frac{d}{dr} \\ -\frac{\alpha}{K}\frac{1}{r}\frac{d}{dr}(r) & \frac{1}{r}\frac{d}{dr}\left(r\frac{d}{dr}\right) - \frac{S_P}{K} \end{pmatrix}$$

is the differential operator of the second order, and

$$A_0 = \begin{pmatrix} \frac{\kappa+1}{2\kappa-2} & 0 \\ 0 & 0 \end{pmatrix}, B_0 = \begin{pmatrix} \frac{3-\kappa}{2\kappa-2} & 0 \\ 0 & 1 \end{pmatrix}, \vec{g}_0 = \begin{pmatrix} \frac{L_0}{2} - \alpha P_0 \\ P_0 \end{pmatrix}.$$

The vector boundary value problem (8) is solved with the help of matrix differential calculation similarly to (4). The corresponding matrix differential equation

$$\tilde{L}_2 Y_0(r) = 0 \tag{9}$$

is considered. Here $Y_0(r)$ is a 2×2 matrix. The correspondence $\tilde{L}_2 H_0(r, \xi) = -H_0(r, \xi) M_0(\xi)$ is used, where

$$H_0(r, \xi) = \begin{pmatrix} Y_1(\xi r) & 0 \\ 0 & Y_0(\xi r) \end{pmatrix}, \quad M_0(\xi) = \begin{pmatrix} \xi^2 & -\alpha \frac{\kappa-1}{\kappa+1} \xi \\ \frac{\alpha}{K} \xi & \xi^2 + \frac{S_P}{K} \end{pmatrix}.$$

The solution of the matrix differential equation (9), according to [6], is received by the formula

$$Y_0(r) = \frac{1}{2\pi \mathrm{i}} \oint_{C_0} H_0(r, \xi) M_0^{-1}(\xi) d\xi, \tag{10}$$

where $M_0^{-1}(\xi)$ is the inverse matrix to $M_0(\xi)$, the closed contour C_0 covers all singularity points of the matrix $M_0^{-1}(\xi)$, which are $\xi = 0, \xi = \pm i \sqrt{\frac{\frac{\alpha^2(\kappa-1)}{\kappa+1} + S_P}{K}}$. Calculation of the contour integral (10) was done with the help of residual theorem. The system of fundamental matrix solutions $Y_{0,i}(r), i = \overline{1,3}$ is derived. The solution of the vector boundary value problem (8) can be written in the form

$$\vec{y}_0(r) = (Y_{0,1}(r) + Y_{0,2}(r)) \begin{pmatrix} c_{0,1} \\ c_{0,2} \end{pmatrix}, \tag{11}$$

where $c_{0,i}, i = \overline{1,2}$ are constants found from the boundary conditions in (8).

The application of the inverse Fourier transform formula [14] to the derived solutions (7), (11) completes solving the original problem (1)–(3).

4. Graphical results

The resulting exact formulae for stress and displacements of layer points provide indications of changes in elastic characteristics and pore pressure. For this purpose, a numerical study was carried out and is discussed below.

The investigation of stress and pore pressure $\sigma_r(r, z), p(r, z)$ was provided for 3 different poroelastic materials [4]: 1) Charcoal granite ($G = 1.87 \cdot 10^{10}, \mu = 0.27, \alpha = 0.242, k = 1 \cdot 10^{-16}, S_p = 1.377 \cdot 10^{-11}$); 2) Westerly granite ($G = 1.5 \cdot 10^{10}, \mu = 0.25, \alpha = 0.449, k = 4 \cdot 10^{-16}, S_p = 1.412 \cdot 10^{-11}$); 3) Ruhr sandstone ($G = 1.33 \cdot 10^{10}, \mu = 0.12, \alpha = 0.637, k = 2 \cdot 10^{-13}, S_p = 2.604 \cdot 10^{-11}$) and 3 different types of a load applied at the surface $r = a$:
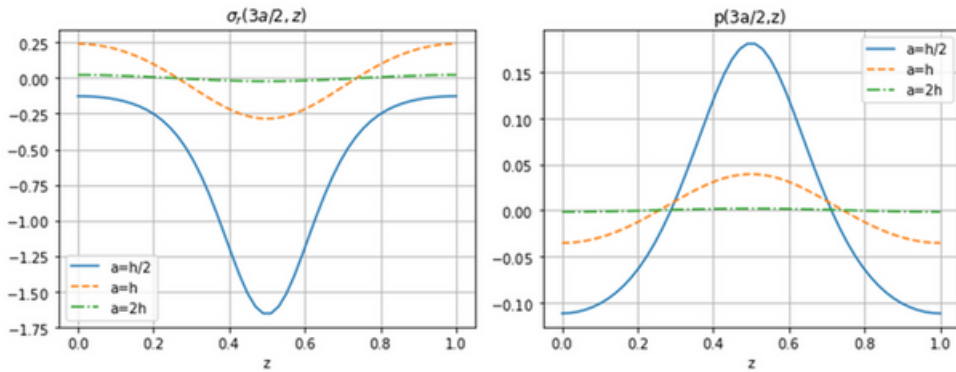
FIGURE 2. The distribution of normal stress and pore pressure values regarding the change of the hole's radius. The case with concentrated normal loading.

1) concentrated normal loading $L(z) = \delta(z - h/2), T(z) = 0, P(z) = 0$; 2) distributed normal loading $L(z) = \sin \pi z/h, T(z) = 0, P(z) = 0$; 3) distributed tangential loading $L(z) = 0, T(z) = \sin \pi z/h, P(z) = 0$.

The Figure 2 shows the change of normal stress σ_r and pore pressure p regarding the change of the hole's radius a for the concentrated normal loading. Here the height of the cylinder $h = 1$. As it can be seen, the maximal absolute values of normal stress and pore pressure are observed at the point $z = h/2$ where the load is applied. Tensile stress is seen closer to the top and bottom surfaces of the layer only when the size of the radius is greater than the height $a \geq h$.
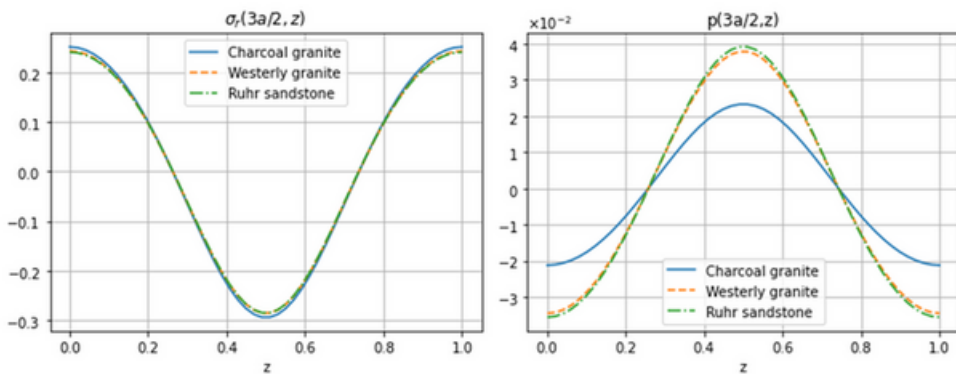

FIGURE 3. The distribution of normal stress and pore pressure values regarding the change of the poroelastic material. The case with concentrated normal loading.

The influence of poroelastic material's change on the values of normal stress σ_r and pore pressure is presented in Figure 3. Here the values of normal stress for three chosen materials are very close while pore pressure values change significantly. The least absolute values of pore pressure are observed for the material with the smallest Biot's coefficient.

The case for the distributed normal loading is shown at Figures 4–5. The similar patterns are observed here, but the absolute values of normal stress and pore pressure are less than for the case of concentrated normal loading.
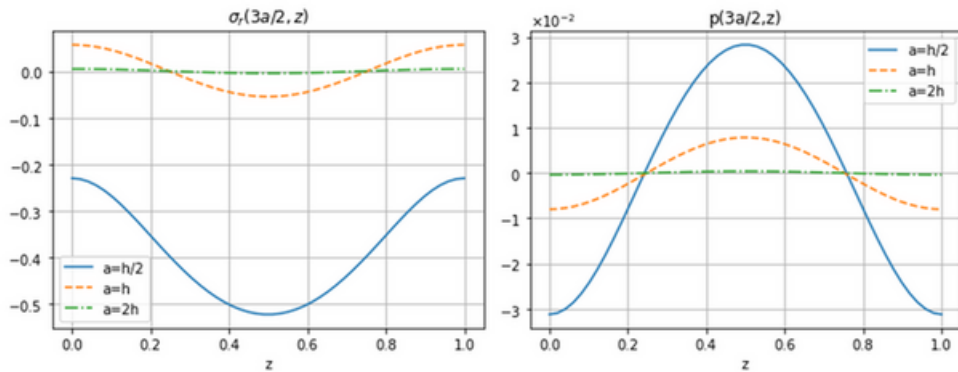

FIGURE 4. The distribution of normal stress and pore pressure values regarding the change of the hole's radius. The case with distributed normal loading.
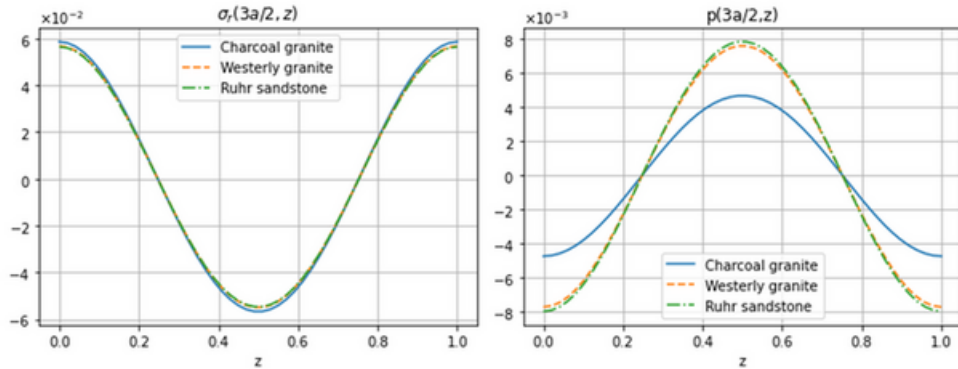

FIGURE 5. The distribution of normal stress and pore pressure values regarding the change of the poroelastic material. The case with distributed normal loading.

5. Conclusions

The exact solution of the problem for a poroelastic layer with a cylindrical hole is derived with the help of integral transform method and matrix differential calculation.

The porous stress state of the layer was investigated regarding different poroelastic materials and geometric sizes of the cylindrical hole.

The proposed approach can be used to solve porothermoelastic problems and poroelastic problems for the layer with cracks.

Acknowledgements

References

[1] H. Arif and J. Lellep, *Stability of nanobeams and nanoplates with defects*, Acta Comment. Univ. Tartu. Math. **25** (2021), 221–238. DOI

[2] B. Babajanov and F. Abdikarimov, *New exact soliton and periodic wave solutions of the nonlinear fractional evolution equations with additional term*, Partial Differ. Equ. Appl. Math. **8** (2023), 5 pp. DOI

[3] M. A. Biot, *General theory of three-dimensional consolidation*, J. Appl. Phys. **12** (1941), 155–164. DOI

[4] A. H.-D. Cheng, *Poroelasticity, Theory and Applications of Transport in Porous Media* **27**, Springer, 2016. DOI

[5] M. V. Dudyk and L. A. Kipnis, *Model of the structure of the near tip area of interface crack in a piece-homogeneous elastic-plastic body*, Strength, Fracture and Complexity **11** (2018), 31–50. DOI

[6] F.-R. Gantmacher, *The Theory of Matrices*, Chelsea Publishing Company, New York, 1959.

[7] H. Hein and L. Jaanuska, *Comparison of machine learning methods for crack localization*, Acta Comment. Univ. Tartu. Math. **23** (2019), 125–142. DOI

[8] F. Karpfinger, B. Gurevich, H.-P. Valero, A. Bakulin, and B. Sinha, *Tube wave signatures in cylindrically layered poroelastic media computed with spectral method*, Geophys. J. International **183** (2010), 1005–1013. DOI

[9] C. Lagarrigue, J. P. Groby, V. Tournat, O. Dazel, and O. Umnova, *Absorption of sound by porous layers with embedded periodic arrays of resonant inclusions*, J. Acoust. Soc. Am. **134** (2013), 4670–4680. DOI

[10] O. Menshykov, M. Menshykova, and N. Vaysfeld, *Exact analytical solution for a pie shaped wedge thick plate under oscillating load*, Acta Mechanica **228** (2017), 4435–4450. DOI

[11] M. Nespoli, M. E. Belardinelli, and M. Bonafede, *Stress and deformation induced in layered media by cylindrical thermo-poro-elastic sources: An application to Campi Flegrei (Italy)*, J. Volcanol. Geotherm. Res. **415** (2021), 14 pp. DOI

[12] G. Ya. Popov, *Exact Solutions of Some Boundary Problems of Deformable Solid Mechanic*, Astroprint, Odessa, 2013. (Russian)

[13] H. Qi, Y. Zhang, F. Chu, and J. Guo, *Scattering of SH waves by a partially debonded cylindrical inclusion in the covering layer*, Mathematical Problems in Engineering **2020** (2020), 13 pp. DOI

[14] E. C. Titchmarsh, *Introduction to the Theory of Fourier Intergrals*, Oxford University Press, Oxford, 1948.

[15] N. Vaysfeld and Z. Zhuravlova, *Exact solution of the axisymmetric problem for poroelastic finite cylinder*. In: Altenbach et al. (eds) Solid Mechanics, Theory of Elasticity and Creep. Advanced Structured Materials, Springer, Cham, 2023, 361–373. DOI

[16] A. Verruijt, *An Introduction to Soil Dynamics, Theory and Applications of Transport in Porous Media* **24**, Springer, 2010. DOI

[17] T. Weisser, J.-Ph. Groby, O. Dazel, F. Gaultier, E. Deckers, S. Futatsugi, and L. Monteiro, *Acoustic behavior of a rigidly backed poroelastic layer with periodic resonant inclusions by a multiple scattering approach*, J. Acoust. Soc. Am. **139** (2016), 617–629. DOI

[18] Z. Yang and X. Zou, *An analytical solution for the horizontal vibration behavior of a cylindrical rigid foundation in poroelastic soil layer*, J. International Association for Earthq. Eng. **52** (2023), 1617–1628.

King's college, Strand building, S2.35, London, United Kingdom
E-mail address: natalya.vaysfeld@kcl.ac.uk

Odesa I.I. Mechnikov National University, Faculty of Mathematics, Physics and Information Technologies, Dvoryanska Str. 2, Odesa 65082, Ukraine
E-mail address: z.zhuravlova@onu.edu.ua